Mathematical Biosciences and Engineering

http://www.aimspress.com/journal/mbe

MBE, 19(10): 10078–10095.
DOI: 10.3934/mbe.2022471
Received: 13 April 2022
Revised: 09 June 2022
Accepted: 10 June 2022
Published: 15 July 2022

Research article

Partition dimension of COVID antiviral drug structures

Ali Al Khabyah[1], Muhammad Kamran Jamil[2], Ali N. A. Koam[1], Aisha Javed[3] and Muhammad Azeem[2,*]

[1] Department of Mathematics, College of Science, Jazan University, New Campus, Jazan 2097, Saudi Arabia

[2] Department of Mathematics, Riphah Institute of Computing and Applied Sciences, Riphah International University Lahore, Pakistan

[3] Abdus Salam School of Mathematical Sciences, Government College University, Lahore, Pakistan

* **Correspondence:** Email: azeemali7009@gmail.com; Tel: +923005067913.

Abstract: In November 2019, there was the first case of COVID-19 (Coronavirus) recorded, and up to 3rd of April 2020, 1,116,643 confirmed positive cases, and around 59,158 dying were recorded. Novel antiviral structures of the SARS-COV-2 virus is discussed in terms of the metric basis of their molecular graph. These structures are named arbidol, chloroquine, hydroxy-chloroquine, thalidomide, and theaflavin. Partition dimension or partition metric basis is a concept in which the whole vertex set of a structure is uniquely identified by developing proper subsets of the entire vertex set and named as partition resolving set. By this concept of vertex-metric resolvability of COVID-19 antiviral drug structures are uniquely identified and helps to study the structural properties of structure.

Keywords: COVID antiviral drug structure; vertex metric dimension; partition dimension; partition locating number; partition locating set

1. Introduction

Cholera, flu and plague were the most terrifying pandemics in the past few centuries, these diseases caused millions of inhabitants of this world to die. The first incidence of COVID-19 (Coronavirus) was reported in November 2019, and by the third week of April 2020, there had been 1,116,643 confirmed positive cases and roughly 59,158 deaths. These statistics are given by the world health Organization (WHO). Not only the human health infected by this pandemic but also the economy of the world was disrupted because it spread over the world after emerging from the seafood market of Wuhan city in China [1]. The viral structure and genetic sequence of betacoronavirus (MERS-CoV) also known as novel corona or 2019-nCoV shares with the MERS-CoV which is middle eastern respiratory syndrome

coronavirus. As there are some specific drugs available for this pandemic virus currently, like Pfizer. To tackle this pathogen there is an urgent need for strong antiviral agents. Researchers experimented with some existing antiviral operatives [2–6] and obtained some productive outcomes to tackle the transmission and infection of COVID-19. Theaflavin, hydroxychloroquine, chloroquine, thalidomide and arbidol are some antiviral compounds.

Remdesivir (GS5734) helped to prevent the infection of the Ebola virus, having a broad spectrum activity as a nucleotide analog drug [7]. It is reported in [8, 9], that chloroquine is considered an antiviral drug that is also broad-spectrum. This antiviral helps to prevent autoimmune disease and malaria. This antiviral tested for the treatment of corona-virus to lower the impact of infections of fever and later on this was found helpful. By inhibiting T cell activation, hydroxy-chloroquine supposed by cytokine storm conclusively reduces the acute evolution of COVID-19. Hydroxychloroquine and chloroquine are approved by FDA as an emergency corona-virus treatment on 30^{rd} march of 2020, reported by Forbes [10]. The inhibitor production of corona-virus by using theaflavin as a lead compound is researched and suggested by [4]. For hepatitis C, B, A viruses and influenza, theaflavin shows a vast span of antiviral activity [11, 12]. For the medical benefit of black tea, a polyphenol chemical is found liable.

By a molecular graph in this draft, we consider a transformation from a chemical structure to a molecular graph by assuming atoms and chemical bonds between them are nodes and edges respectively, and this theory is already established, for more detail, one can view some recent literature [13–17].

Definition 1.1. In [18]*" Suppose* $\aleph(V(\aleph), E(\aleph))$ *is an undirected graph of a chemical structure (network) with* $V(\aleph)$ *is called as set of principal nodes (vertex set) and* $E(\aleph)$ *is the set of branches (edge set). The distance between two principal nodes* $\zeta_1, \zeta_2 \in V(\aleph)$, *denoted as* $d(\zeta_1, \zeta_2)$ *is the minimum count of branches between* $\zeta_1 - \zeta_2$ *path."*

Definition 1.2. In [18] *"Suppose* $R \subset V(\aleph)$ *is the subset of principal nodes set and defined as* $R = \{\zeta_1, \zeta_2, \ldots, \zeta_s\}$, *and let a principal node* $\zeta \in V(\aleph)$. *The identification or locations* $r(\zeta|R)$ *of a principal node* ζ *with respect to R is actually a* $s-$*ordered distances* $(d(\zeta, \zeta_1), d(\zeta, \zeta_2), \ldots, d(\zeta, \zeta_s))$. *If each principal node from* $V(\aleph)$ *have unique identification according to the ordered subset R, then this subset renamed as a resolving set of network* $\aleph$. *The minimum numbers of the elements in the subset R is actually the metric dimension of* $\aleph$ *and it is denoted by the term* $dim(\aleph)$."

Definition 1.3. In [19] *"Let* $R_p \subseteq V(\aleph)$ *is the s-elements proper set and* $r\left(\zeta|R_p\right) = \{d(\zeta, R_{p1}), d(\zeta, R_{p2}), \ldots, d(\zeta, R_{ps})\}$, *is the s-tuple distance identification of a principal node* ζ *in association with* R_p. *If the entire set of principal nodes have unique identifications, then* R_p *is named as the partition resolving set of the principal node of a network* $\aleph$. *The least possible count of the subsets in that set of* $V(\aleph)$ *is labeled as the partition dimension* $(pd(\aleph))$ *of* $\aleph$."

In the above definitions a graph or a chemical structure is shown with symbol $\aleph$, notation $r(\zeta|R)$ shows the position of a vertex ζ with respect to the resolving set or locating set R, and for the partition resolving set they used the symbol R_p, $dim(\aleph)$ is used for the metric dimension of a graph $\aleph$, partition dimension is notated by the symbol $pd(\aleph)$, furthermore, the notations are summarized in the Table 1.

Very few and recent literature on the topic of metrics and their generalization are given here. In [20], polycyclic aromatic compounds are discussed on the topic of metric and its generalization. A chemical

structure is discussed in [21], they mentioned two-dimensional lattice is discussed with the idea of metric and of that structure. Cellulose network is considered in [22], by the same concept of distance-based theory of graph. Generalized concepts are given by [23–26]. A computer network is discussed in [27] with the concept of distance graph theory. Generalized families and structures of the graph are detailed in [28–32].

Table 1. Basic notions.

Terminologies	Notations
Structure	$G_{Structure}$
Vertex set	$V(G_{Structure})$
Edge set	$E(G_{Structure})$
locating set	ls
locating number	ln
partition locating set	lsp
partition locating number	pln
location of a vertex with respect to partition locating set v	$l(v\|lsp)$

The partition dimension is quite a complex structure than the metric dimension, therefore, fewer exact partitions are available and bounds are presented usually. In [33], presented bounds for the partition of generalized class of convex polytopes and also in [34]. A chemical fullerene graph is presented in [35] and bounds on another chemical structure are detailed in [36], some nanotubes and sheets are presented in the form of partition sets in [37], the two-dimensional lattice structure is available in [38]. Generalized structures and classes of families of graphs are detailed in [39–45].

The very first use of metric dimension in 1975 by Slater [46] and he named this concept as locating set. Later in 1976, two independent researchers from the computer science field named this concept as the resolving set found in [47]. This idea is also named the metric basis in the pure mathematical study of graphs and structures, available in [48,49]. Instead of choosing a single subset from the vertex set of a graph or structure, the researchers of [49], introduced a concept in which a vertex set is completely arranged in the different disjoint subsets in such a manner to get unique identifications of vertices, and this concept is known as partition resolving set or partition dimension.

Metric dimension has many applied ways in which combinatorial optimization, robot roving, in complex games, image processing, pharmaceutical chemistry, polymer industry, and in the electric field as well. All these applications are found in [19, 46, 50–52]. Robot roving is also attached with the concept of applications of the partitioning of a vertex set in terms of metric [50], while Djokovic-Winkler relation [53], verification, and discovery of a network, in chemistry [54], in mastermind games [55], image processing, and pattern recognition, and in hierarchical of the data structure are linked to the partition dimensions of a structure [56]. Further applications can be found in the literature of [47, 57].

2. Main results

In this section, we will include our main results of partition locating set of some structures, for example, arbidol, chloroquine, hydroxy-chloroquine, thalidomide and theaflavin.

Given below are the node and bond set of arbidol COVID antiviral drug structure. The order (total count of nodes) and size (total count of edges) of this arbidol structure is $|V(G_{\text{Arbidol}})| = 29$, $|E(G_{\text{Arbidol}})| = 31$, respectively. Moreover, the molecular graph of Arbidol and labeling used in our main results are shown in the Figure 1. Some of the topological properties of this structure are available in the reference [58, 59].

$$V(G_{\text{Arbidol}}) = \{\varpi_i : i = 1, 2, \ldots, 29\}$$
$$E(G_{\text{Arbidol}}) = \{\varpi_i\varpi_{i+1} : i = 1, 2, \ldots, 13,\ i = 15, 16, \ldots, 22,\ i = 24, 25\} \cup \{\varpi_2\varpi_{16},\ \varpi_4\varpi_{18},\ \varpi_5\varpi_{29},\ \varpi_6\varpi_{19},\ \varpi_9\varpi_{14},\ \varpi_{20}\varpi_{28},\ \varpi_{17}\varpi_{24},\ \varpi_{25}\varpi_{27}\}.$$

Theorem 2.1. *Let $G_{Arbidol}$ be a graph of arbidol COVID antiviral drug structure. Then the partition locating number of $G_{Arbidol}$ is less than or equal to four.*

Proof. The partition locating number or partition dimension of graph of arbidol COVID antiviral drug structure is less than or equal to four. To prove this statement we have chosen a partition locating set with cardinality four and stated as $lsp(G_{\text{Arbidol}}) = \{lsp_1, lsp_2, lsp_3, lsp_4\}$, where $lsp_1 = \{\varpi_{10}\}$, $lsp_2 = \{\varpi_{23}\}$, $lsp_3 = \{\varpi_{27}\}$, and $lsp_4 = V(G_{\text{Arbidol}}) \setminus \{\varpi_{10}, \varpi_{23}, \varpi_{27}\}$. Now to make this statement valid we have provided the representations of each node of the arbidol COVID antiviral drug structure which are given in the Table 2.

Table 2. Locations of the nodes of G_{Arbidol}.

$l(\varpi\|lsp)$	lsp_1	lsp_2	lsp_3	lsp_4	i-range
ϖ_i	$10-i$	$10-i$	6	0	$i = 1, 3$
ϖ_i	$10-i$	$10-i$	5	0	$i = 2, 4$
ϖ_i	$10-i$	$i+1$	6	0	$i = 5$
ϖ_i	$10-i$	$i-1$	i	z_1	$i = 6, \ldots, 10$
ϖ_i	$i-10$	$i-1$	i	0	$i = 11, 12$
ϖ_i	$10-i$	$23-i$	$24-i$	0	$i = 13$
ϖ_i	$i-12$	$23-i$	$24-i$	0	$i = 14$
ϖ_i	$10-i$	$i-1$	i	0	$i = 15, 16, 17$
ϖ_i	$24-i$	$23-i$	$i-14$	0	$i = 18, 19$
ϖ_i	$i-14$	$23-i$	$i-14$	z_1	$i = 20, 21, 22, 23$
ϖ_i	$i-16$	$i-17$	2	0	$i = 24, 26$
ϖ_i	$i-16$	$i-17$	1	0	$i = 25$
ϖ_i	10	9	0	1	$i = 27$
ϖ_i	$35-i$	4	7	0	$i = 28$
ϖ_i	$35-i$	7	7	0	$i = 29$

where $z_1 = \begin{cases} 1, & \text{if } i = 10, 23; \\ 0, & \text{otherwise.} \end{cases}$

Given locations $l(\varpi|lsp)$ of each node of graph of arbidol COVID antiviral drug structure is distinct and fulfill the definitions of partition locating set. This proved that the partition locating number $pln(G_{\text{Arbidol}}) \leq 4$ of graph of arbidol COVID antiviral drug structure.

Hence, proved that $pln(G_{\text{Arbidol}}) \leq 4$. □

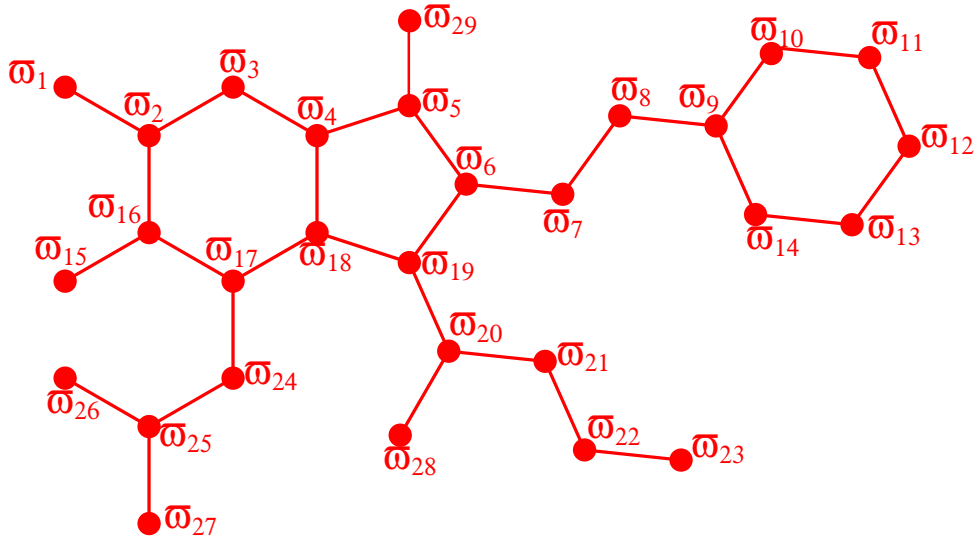

Figure 1. Arbidol COVID antiviral drug structure.

Given below are the node and bond set of chloroquine COVID antiviral drug structure. The order (total count of nodes) and size (total count of edges) of this chloroquine structure is $\left|V\left(G_{\text{Chloroquine}}\right)\right| = 22$, $\left|E\left(G_{\text{Chloroquine}}\right)\right| = 23$, respectively. Moreover, the molecular graph of Chloroquine and labeling used in our main results are shown in the Figure 2. Some of the topological properties of this structure are available in the reference [58, 59].

$$V\left(G_{\text{Chloroquine}}\right) = \{\varpi_i : i = 1, 2, \ldots, 22\}$$

$$E\left(G_{\text{Chloroquine}}\right) = \{\varpi_i\varpi_{i+1} : i = 1, 2, \ldots, 13,\ i = 15,\ i = 17, \ldots, 20\} \cup \{\varpi_2\varpi_{21},\ \varpi_5\varpi_{20},\ \varpi_6\varpi_{17},\ \varpi_8\varpi_{22},\ \varpi_{12}\varpi_{15}\}.$$

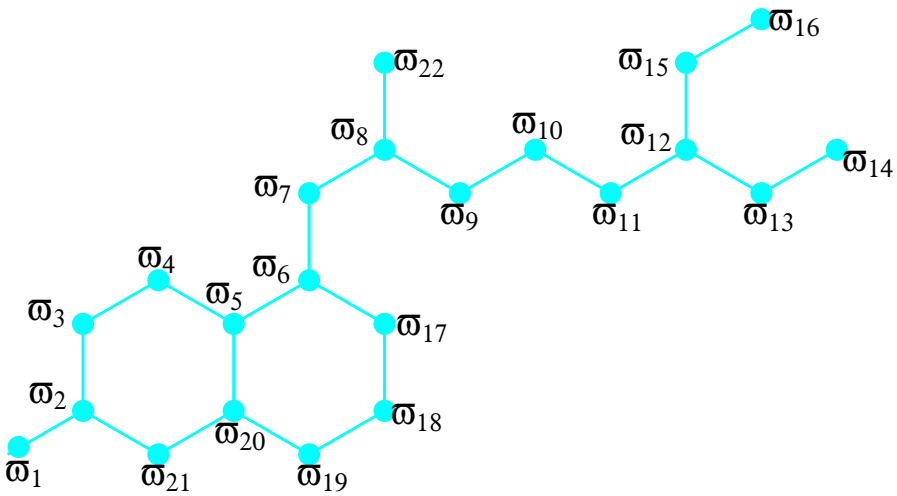

Figure 2. Chloroquine COVID antiviral drug structure.

Theorem 2.2. *Let $G_{Chloroquine}$ be a graph of chloroquine COVID antiviral drug structure. Then the partition locating number of $G_{Chloroquine}$ is three.*

Proof. The partition locating number or partition dimension of graph of chloroquine COVID antiviral drug structure is three. To prove this statement we have chosen a partition locating set with cardinality three and stated as $lsp\left(G_{\text{Chloroquine}}\right) = \{lsp_1,\ lsp_2,\ lsp_3\}$, where $lsp_1 = \{\varpi_3\},\ lsp_2 = \{\varpi_{14}\}$, and $lsp_3 = V\left(G_{\text{Chloroquine}}\right) \setminus \{\varpi_3,\ \varpi_{14}\}$. Now to make this statement valid we have provided the representations of each node of the chloroquine COVID antiviral drug structure which are given in the Table 3.

Table 3. Locations of the nodes of $G_{\text{Chloroquine}}$.

$l(\varpi\|lsp)$	lsp_1	lsp_2	lsp_3	i-range
ϖ_i	$\|i-3\|$	$14-i$	z_2	$i = 1, 2, \ldots, 14$
ϖ_i	$i-5$	$i-12$	0	$i = 15, 16$
ϖ_i	$i-13$	$i-8$	0	$i = 17$
ϖ_i	$23-i$	$i-8$	0	$i = 18, 19$
ϖ_i	$23-i$	$i-10$	0	$i = 20, 21$
ϖ_i	$i-18$	$i-15$	0	$i = 22$

where $z_2 = \begin{cases} 1, & \text{if } i = 3, 14; \\ 0, & \text{otherwise.} \end{cases}$

Given locations $l(\varpi|lsp)$ of each node of graph of chloroquine COVID antiviral drug structure is distinct and fulfill the definitions of partition locating set. This proved that the partition locating number $pln\left(G_{\text{Chloroquine}}\right) \leq 3$ of graph of chloroquine COVID antiviral drug structure. To make this assertion exact we need to prove that $pln\left(G_{\text{Chloroquine}}\right) \geq 3$ and following by contradiction we will have $pln\left(G_{\text{Chloroquine}}\right) = 2$. Now, this is not true because this statement is reserved for path graph.

Hence, proved that $pln\left(G_{\text{Chloroquine}}\right) = 3$. □

Given below are the node and bond set of hydroxy-chloroquine COVID antiviral drug structure. The order (total count of nodes) and size (total count of edges) of this hydroxy-chloroquine structure is $\left|V\left(G_{\text{Hydroxy}}\right)\right| = 23$, $\left|E\left(G_{\text{Hydroxy}}\right)\right| = 24$, respectively. Moreover, the molecular graph of hydroxy-chloroquine and labeling used in our main results are shown in the Figure 3. Some of the topological properties of this structure are available in the reference [58, 59].

$$\begin{aligned} V\left(G_{\text{Hydroxy}}\right) =& \{\varpi_i :\ i = 1, 2, \ldots, 23\} \\ E\left(G_{\text{Hydroxy}}\right) =& \{\varpi_i\varpi_{i+1} :\ i = 1, 2, \ldots, 13,\ i = 15, 16,\ i = 18, \ldots, 21\} \cup \{\varpi_2\varpi_{22},\ \varpi_5\varpi_{21}, \\ & \varpi_6\varpi_{18},\ \varpi_8\varpi_{23},\ \varpi_{12}\varpi_{15}\}. \end{aligned}$$

Theorem 2.3. *Let $G_{Hydroxy}$ be a graph of hydroxy-chloroquine COVID antiviral drug structure. Then the partition locating number of $G_{Hydroxy}$ is three.*

Proof. The partition locating number or partition dimension of graph of hydroxy-chloroquine COVID antiviral drug structure is three. To prove this statement we have chosen a partition locating set with

cardinality three and stated as $lsp\left(G_{\text{Hydroxy}}\right) = \{lsp_1,\ lsp_2,\ lsp_3\}$, where $lsp_1 = \{\varpi_3\},\ lsp_2 = \{\varpi_{14}\}$, and $lsp_3 = V\left(G_{\text{Hydroxy}}\right)\backslash\{\varpi_3,\ \varpi_{14}\}$. Now to make this statement valid we have provided the representations of each node of the hydroxy-chloroquine COVID antiviral drug structure which are given in the Table 4.

Table 4. Locations of the nodes of G_{Hydroxy}.

$l(\varpi\|lsp)$	lsp_1	lsp_2	lsp_3	i-range
ϖ_i	$\|i-3\|$	$14-i$	z_3	$i = 1, 2, \ldots, 14$
ϖ_i	$i-5$	$i-12$	0	$i = 15, 16, 17$
ϖ_i	$i-14$	$i-9$	0	$i = 18$
ϖ_i	$24-i$	$i-9$	0	$i = 19, 20$
ϖ_i	$24-i$	$i-11$	0	$i = 21, 22$
ϖ_i	$i-17$	$i-16$	0	$i = 23$

where $z_3 = \begin{cases} 1, & \text{if } i = 3, 14; \\ 0, & \text{otherwise.} \end{cases}$

Given locations $l(\varpi|lsp)$ of each node of graph of hydroxy-chloroquine COVID antiviral drug structure is distinct and fulfill the definitions of partition locating set. This proved that the partition locating number $pln\left(G_{\text{Hydroxy}}\right) \leq 3$ of graph of hydroxy-chloroquine COVID antiviral drug structure. To make this assertion exact we need to prove that $pln\left(G_{\text{Hydroxy}}\right) \geq 3$ and following by contradiction we will have $pln\left(G_{\text{Hydroxy}}\right) = 2$. Now, this is not true because this statement is reserved for path graph.

Hence, proved that $pln\left(G_{\text{Hydroxy}}\right) = 3$. □

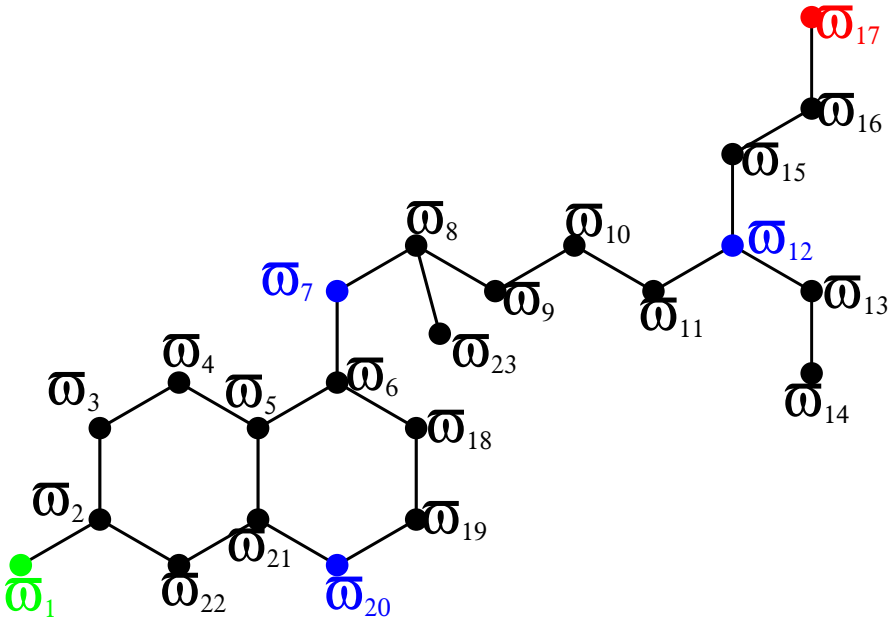

Figure 3. Hydroxy-Chloroquine COVID antiviral drug structure.

Given below are the node and bond set of thalidomide COVID antiviral drug structure. The order (total count of nodes) and size (total count of edges) of this thalidomide structure is $|V(G_{\text{Thalidomide}})| = 19$, $|E(G_{\text{Thalidomide}})| = 21$, respectively. Moreover, the molecular graph of Thalidomide and labeling used in our main results are shown in the Figure 4. Some of the topological properties of this structure are available in the reference [58, 59].

$$V(G_{\text{Thalidomide}}) = \{\varpi_i : i = 1, 2, \ldots, 19\}$$

$$E(G_{\text{Thalidomide}}) = \{\varpi_i\varpi_{i+1} : i = 1, 2, \ldots, 14,\ i = 16\} \cup \{\varpi_2\varpi_{17},\ \varpi_4\varpi_{19},\ \varpi_7\varpi_{18},\ \varpi_5\varpi_{16},\ \varpi_6\varpi_{14},\ \varpi_8\varpi_{13}\}.$$

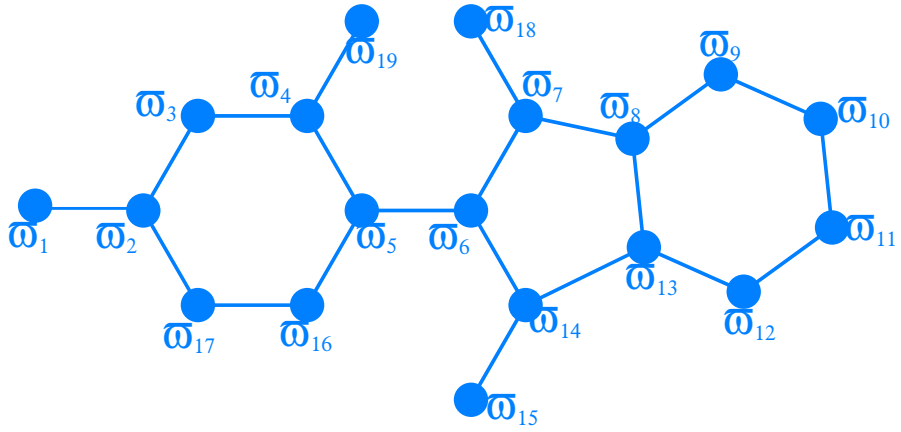

Figure 4. Thalidomide COVID antiviral drug structure.

Theorem 2.4. *Let $G_{Thalidomide}$ be a graph of Thalidomide COVID antiviral drug structure. Then the partition locating number of $G_{Thalidomide}$ is three.*

Proof. The partition locating number or partition dimension of graph of Thalidomide COVID antiviral drug structure is three. To prove this statement we have chosen a partition locating set with cardinality three and stated as $lsp(G_{\text{Thalidomide}}) = \{lsp_1, lsp_2, lsp_3\}$, where $lsp_1 = \{\varpi_6\}$, $lsp_2 = \{\varpi_{18}\}$, and $lsp_3 = V(G_{\text{Thalidomide}}) \setminus \{\varpi_6, \varpi_{18}\}$. Now to make this statement valid we have provided the representations of each node of the Thalidomide COVID antiviral drug structure which are given in the Table 5.

Table 5. Locations of the nodes of $G_{\text{Thalidomide}}$.

$l(\varpi\|lsp)$	lsp_1	lsp_2	lsp_3	i-range
ϖ_i	$\|i-6\|$	$\|7-i\|+1$	z_4	$i = 1, 2, \ldots, 10$
ϖ_i	$15-i$	$16-i$	0	$i = 12, 13$
ϖ_i	$15-i$	$i-13$	0	$i = 14$
ϖ_i	2	$i-13$	0	$i = 15$
ϖ_i	$i-14$	$i-12$	0	$i = 16, 17$
ϖ_i	$i-16$	$i-18$	1	$i = 18$
ϖ_i	$i-16$	$i-14$	0	$i = 19$

where $z_4 = \begin{cases} 1, & \text{if } i = 6; \\ 0, & \text{otherwise.} \end{cases}$

Given locations $l(\varpi|lsp)$ of each node of graph of Thalidomide COVID antiviral drug structure is distinct and fulfill the definitions of partition locating set. This proved that the partition locating number $pln(G_{\text{Thalidomide}}) \leq 3$ of graph of Thalidomide COVID antiviral drug structure. To make this assertion exact we need to prove that $pln(G_{\text{Thalidomide}}) \geq 3$ and following by contradiction we will have $pln(G_{\text{Thalidomide}}) = 2$. Now, this is not true because this statement is reserved for path graph.

Hence, proved that $pln(G_{\text{Thalidomide}}) = 3$. □

Given below are the node and bond set of theaflavin COVID antiviral drug structure. The order (total count of nodes) and size (total count of edges) of this theaflavin structure is $|V(G_{\text{Theaflavin}})| = 41$, $|E(G_{\text{Theaflavin}})| = 46$, respectively. Moreover, the molecular graph of Theaflavin and labeling used in our main results are shown in the Figure 5. Some of the topological properties of this structure are available in the reference [58, 59].

$$V(G_{\text{Theaflavin}}) = \{\varpi_i : i = 1, 2, \ldots, 41\}$$

$$E(G_{\text{Theaflavin}}) = \{\varpi_i\varpi_{i+1} : i = 1, 2, \ldots, 23,\ i = 25, 26, \ldots, 30\} \cup \{\varpi_1\varpi_{39},\ \varpi_1\varpi_{10}, \varpi_3\varpi_8, \varpi_4\varpi_{40},\ \varpi_6\varpi_{41},\ \varpi_{11}\varpi_{31},\ \varpi_{14}\varpi_{25},\ \varpi_{30}\varpi_{38},\ \varpi_{29}\varpi_{37},\ \varpi_{27}\varpi_{36},\ \varpi_{26}\varpi_{35},\ \varpi_{13}\varpi_{28},\ \varpi_{16}\varpi_{34}, \varpi_{15}\varpi_{24},\ \varpi_{18}\varpi_{23},\ \varpi_{22}\varpi_{33},\ \varpi_{20}\varpi_{32}\}.$$

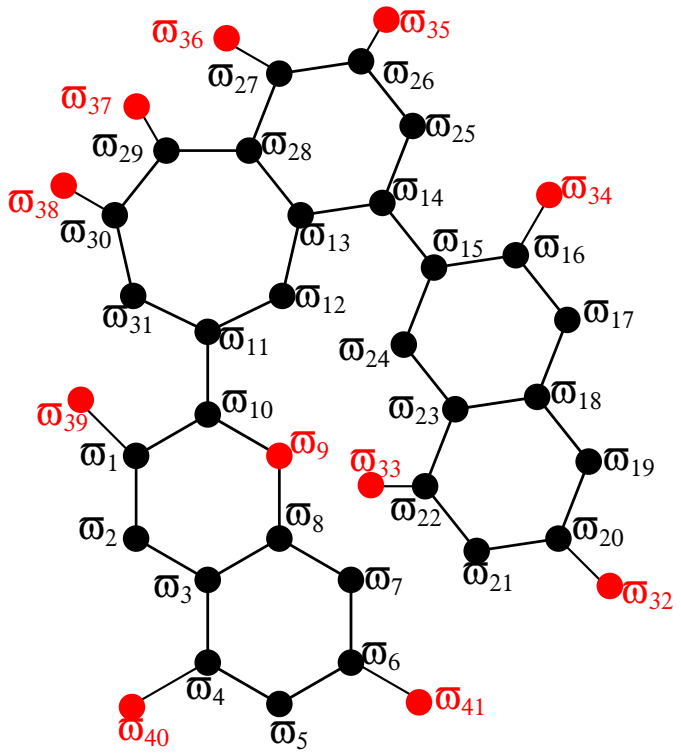

Figure 5. Theaflavin COVID antiviral drug structure.

Theorem 2.5. *Let $G_{Theaflavin}$ be a graph of Theaflavin COVID antiviral drug structure. Then the partition locating number of $G_{Theaflavin}$ is three.*

Proof. The partition locating number or partition dimension of graph of Theaflavin COVID antiviral drug structure is three. To prove this statement we have chosen a partition locating set with cardinality three and stated as $lsp\,(G_{\text{Theaflavin}}) = \{lsp_1,\ lsp_2,\ lsp_3\}$, where $lsp_1 = \{\varpi_{31}\}$, $lsp_2 = \{\varpi_{41}\}$ and $lsp_3 = V\,(G_{\text{Theaflavin}}) \setminus \{\varpi_{31},\ \varpi_{41}\}$. Now to make this statement valid we have provided the representations of each node of the Theaflavin COVID antiviral drug structure which are given in the Table 6.

Table 6. Locations of the nodes of $G_{\text{Theaflavin}}$.

$l\,(\varpi \vert lsp)$	lsp_1	lsp_2	lsp_3	i-range
ϖ_i	$i+9$	$7-i$	0	$i = 1, 2, \ldots, 5$
ϖ_i	$19-i$	$i-5$	0	$i = 6, 7, \ldots, 15$
ϖ_i	$21-i$	$i-5$	0	$i = 16, 17, 18$
ϖ_i	$23-i$	$35-i$	0	$i = 19, 20$
ϖ_i	$23-i$	$35-i$	0	$i = 21, 22$
ϖ_i	$i-21$	$35-i$	0	$i = 23, 24$
ϖ_i	$i-19$	$37-i$	0	$i = 25$
ϖ_i	$i-19$	$37-i$	0	$i = 26, 27$
ϖ_i	$i-21$	$37-i$	0	$i = 28$
ϖ_i	$i-21$	$38-i$	0	$i = 29, 30$
ϖ_i	$i-22$	$38-i$	0	$i = 31$
ϖ_i	$i-28$	$i-16$	0	$i = 32$
ϖ_i	$i-33$	$i-19$	1	$i = 33$
ϖ_i	$i-28$	$i-22$	0	$i = 34$
ϖ_i	$i-27$	$47-i$	0	$i = 35, 36$
ϖ_i	$i-28$	$47-i$	0	$i = 37, 38$
ϖ_i	$i-28$	$i-32$	0	$i = 39$
ϖ_i	$i-26$	$i-36$	0	$i = 40$
ϖ_i	$i-27$	$i-41$	1	$i = 41$

Given locations $l\,(\varpi|lsp)$ of each node of graph of Theaflavin COVID antiviral drug structure is distinct and fulfill the definitions of partition locating set. This proved that the partition locating number $pln\,(G_{\text{Theaflavin}}) \leq 3$ of graph of Theaflavin COVID antiviral drug structure. To make this assertion exact we need to prove that $pln\,(G_{\text{Theaflavin}}) \geq 3$ and following by contradiction we will have $pln\,(G_{\text{Theaflavin}}) = 2$. Now, this is not true because this statement is reserved for path graph.

Hence, proved that $pln\,(G_{\text{Theaflavin}}) = 3$. □

Given below are the node and bond set of Remdesivir COVID antiviral drug structure. The order (total count of nodes) and size (total count of edges) of this Remdesivir structure is $|V\,(G_{\text{Remdesivir}})| = 41$, $|E\,(G_{\text{Remdesivir}})| = 44$, respectively. Moreover, the molecular graph of Remdesivir and labeling used in our main results are shown in the Figure 6. Some of the topological properties of this structure are available in the reference [58, 59].

$V(G_{\text{Remdesivir}}) = \{\varpi_i : i = 1, 2, \ldots, 41\}$

$E(G_{\text{Remdesivir}}) = \{\varpi_i\varpi_{i+1} : i = 1, 2, \ldots, 21,\ i = 23, 25, 28, 29, 31, 33, 34, 35, 36, 38\} \cup \{\varpi_1\varpi_6,$
$\varpi_8\varpi_{41},\ \varpi_8\varpi_{28},\ \varpi_{29}\varpi_{31},\ \varpi_{31}\varpi_{33},\ \varpi_{35}\varpi_{38},\ \varpi_{11}\varpi_{25},\ \varpi_{13}\varpi_{23},\ \varpi_{23}\varpi_{25},\ \varpi_{13}\varpi_{40},\ \varpi_{17}\varpi_{22},$
$\varpi_{14}\varpi_{22},\ \varpi_{18}\varpi_{27}\}.$

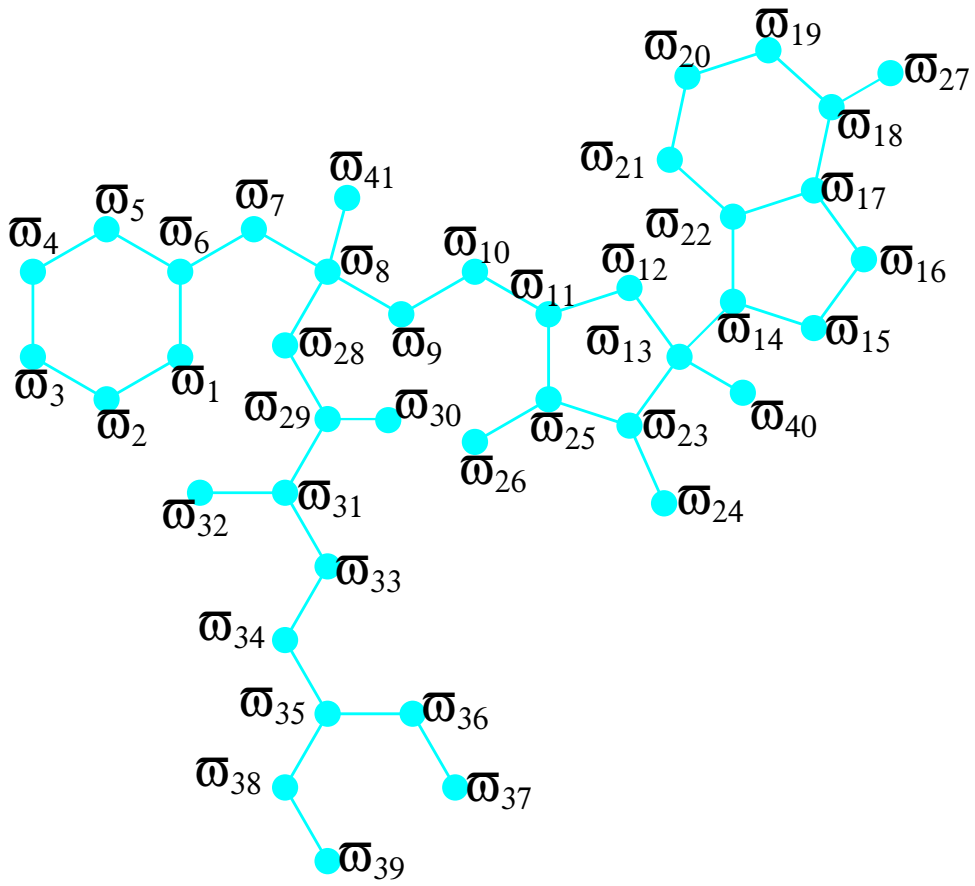

Figure 6. Remdesivir COVID antiviral drug structure.

Theorem 2.6. *Let $G_{Remdesivir}$ be a graph of Remdesivir COVID antiviral drug structure. Then the partition locating number of $G_{Remdesivir}$ is less than or equal to four.*

Proof. The partition locating number or partition dimension of graph of Remdesivir COVID antiviral drug structure is less than or equal to four. To prove this statement we have chosen a partition locating set with cardinality four and stated as $lsp(G_{\text{Remdesivir}}) = \{lsp_1, lsp_2, lsp_3, lsp_4\}$, where $lsp_1 = \{\varpi_4\}$, $lsp_2 = \{\varpi_{27}\}$, $lsp_3 = \{\varpi_{39}\}$, and $lsp_4 = V(G_{\text{Remdesivir}}) \setminus \{\varpi_4, \varpi_{27}, \varpi_{39}\}$. Now to make this statement valid we have provided the representations of each node of the Remdesivir COVID antiviral drug structure which are given in the Table 7.

Table 7. Locations of the nodes of $G_{\text{Remdesivir}}$.

$l(\varpi\|lsp)$	lsp_1	lsp_2	lsp_3	lsp_4	i-range
ϖ_i	$\|4-i\|$	$i+12$	$i+10$	0	$i=1,2,3$
ϖ_i	$\|4-i\|$	$18-i$	$16-i$	z_5	$i=4,5,\ldots,8$
ϖ_i	$\|4-i\|$	$18-i$	$18-i$	0	$i=9,10,\ldots,14$
ϖ_i	$\|4-i\|$	$19-i$	$18-i$	0	$i=15,16$
ϖ_i	$i-5$	$19-i$	$i-1$	0	$i=17,18$
ϖ_i	$i-5$	$i-17$	$i-1$	0	$i=19$
ϖ_i	$33-i$	$i-17$	$37-i$	0	$i=20,21$
ϖ_i	$i-5$	$i-19$	$37-i$	0	$i=22$
ϖ_i	$i-5$	$i-17$	$i-10$	0	$i=23$
ϖ_i	$i-14$	$i-17$	$i-10$	0	$i=24$
ϖ_i	$i-17$	$i-18$	$i-13$	0	$i=25,26$
ϖ_i	$i-13$	$i-27$	$i-9$	1	$i=27$
ϖ_i	$i-23$	$i-17$	$35-i$	0	$i=28,29$
ϖ_i	$i-23$	$i-17$	$i-23$	0	$i=30$
ϖ_i	$i-24$	$i-18$	$i-26$	0	$i=31,32$
ϖ_i	$i-25$	$i-19$	$37-i$	0	$i=33,34,35$
ϖ_i	$i-25$	$i-19$	$i-33$	0	$i=36,37$
ϖ_i	$i-27$	$i-21$	$39-i$	z_5	$i=38,39$
ϖ_i	$i-30$	$i-34$	$i-26$	0	$i=40$
ϖ_i	$i-36$	$i-30$	$i-32$	0	$i=41$

where $z_5 = \begin{cases} 1, & \text{if } i = 4, 39; \\ 0, & \text{otherwise.} \end{cases}$

Given locations $l(\varpi|ls)$ of each node of graph of Remdesivir COVID antiviral drug structure is distinct and fulfill the definitions of partition locating set. This proved that the partition locating number $pln(G_{\text{Remdesivir}}) \leq 4$ of graph of Remdesivir COVID antiviral drug structure.

Hence, proved that $pln(G_{\text{Remdesivir}}) \leq 4$. □

Given below are the node and bond set of Ritonavir COVID antiviral drug structure. The order (total count of nodes) and size (total count of edges) of this Ritonavir structure is $|V(G_{\text{Ritonavir}})| = 50$, $|E(G_{\text{Ritonavir}})| = 53$, respectively. Moreover, the molecular graph of Ritonavir and labeling used in our main results are shown in the Figure 7. Some of the topological properties of this structure are available in the reference [58, 59].

$$V(G_{\text{Ritonavir}}) = \{\varpi_i : i = 1, 2, \ldots, 50\}$$

$$E(G_{\text{Ritonavir}}) = \{\varpi_i\varpi_{i+1} : i = 1, 2, \ldots, 24,\ i = 27, 28, \ldots, 32, 35, 36, \ldots, 40, 43, 48\} \cup$$
$$\{\varpi_{21}\varpi_{25},\ \varpi_{18}\varpi_{26},\ \varpi_{16}\varpi_{27},\ \varpi_{28}\varpi_{33},\ \varpi_{15}\varpi_{34},\ \varpi_{13}\varpi_{35},\ \varpi_{36}\varpi_{41},\ \varpi_{11}\varpi_{42},\ \varpi_{10}\varpi_{43},$$
$$\varpi_{43}\varpi_{45},\ \varpi_7\varpi_{47},\ \varpi_{48}\varpi_{50},\ \varpi_3\varpi_{48},\ \varpi_1\varpi_5\}.$$

Theorem 2.7. *Let $G_{Ritonavir}$ be a graph of Ritonavir COVID antiviral drug structure. Then the partition locating number of $G_{Ritonavir}$ is less than or equal to six.*

Proof. The partition locating number or partition dimension of graph of Ritonavir COVID antiviral drug structure is six. To prove this statement we have chosen a partition locating set with cardinality six and stated as $lsp(G_{\text{Ritonavir}}) = \{lsp_1,\ lsp_2,\ lsp_3,\ lsp_4,\ lsp_5,\ lsp_6\}$, where $lsp_1 = \{\varpi_{22}\}$, $lsp_2 = \{\varpi_{33}\}$, $lsp_3 = \{\varpi_{43}\}$, $lsp_4 = \{\varpi_{44}\}$, $lsp_5 = \{\varpi_{50}\}$, and $lsp_6 = V(G_{\text{Ritonavir}}) \setminus \{\varpi_{22},\ \varpi_{33},\ \varpi_{43},\ \varpi_{44},\ \varpi_{50}\}$. Now to make this statement valid we have provided the representations of each node of the Ritonavir COVID antiviral drug structure which are given in the Table 8.

Table 8. Locations of the nodes of $G_{\text{Ritonavir}}$.

$l(\varpi\|lsp)$	lsp_1	lsp_2	lsp_3	lsp_4	lsp_5	lsp_6	i-range
ϖ_i	$i+17$	$i+14$	$i+6$	$i+7$	$i+2$	0	$i = 1, 2$
ϖ_i	$\|22-i\|$	$19-i$	$11-i$	$12-i$	$i-1$	0	$i = 3, 4, \ldots, 10$
ϖ_i	$\|22-i\|$	$19-i$	$i-9$	$i-8$	$i-1$	0	$i = 11, 12, \ldots, 16$
ϖ_i	$\|22-i\|$	$i-13$	$i-9$	$i-8$	$i-1$	z_6	$i = 17, 18, \ldots, 23$
ϖ_i	$\|22-i\|$	$34-i$	$38-i$	$39-i$	$46-i$	0	$i = 24$
ϖ_i	$i-23$	$34-i$	$38-i$	$39-i$	$46-i$	0	$i = 25$
ϖ_i	$i-21$	$i-20$	$i-16$	$i-15$	$i-8$	0	$i = 26$
ϖ_i	$i-20$	$i-25$	$i-19$	$i-18$	$i-11$	0	$i = 27$
ϖ_i	$i-20$	$i-27$	$i-19$	$i-18$	$i-8$	0	$i = 28, 29, \ldots, 30$
ϖ_i	$i-20$	$33-i$	$i-19$	$i-18$	$i-8$	0	$i = 31$
ϖ_i	$42-i$	$33-i$	$43-i$	$44-i$	$51-i$	z_6	$i = 32, 33$
ϖ_i	$42-i$	$i-29$	$i-27$	$i-28$	$i-19$	0	$i = 34$
ϖ_i	$i-25$	$i-28$	$i-30$	$i-29$	$i-22$	0	$i = 35, 36, \ldots, 39$
ϖ_i	$53-i$	$50-i$	$48-i$	$49-i$	$56-i$	0	$i = 40, 41$
ϖ_i	$i-30$	$i-33$	$i-39$	$i-38$	$53-i$	0	$i = 42$
ϖ_i	$i-30$	$i-33$	$i-43$	$44-i$	$53-i$	1	$i = 43$
ϖ_i	$i-30$	$i-33$	$i-43$	$44-i$	$i-33$	1	$i = 44$
ϖ_i	$i-31$	$i-34$	$i-44$	$i-44$	$i-34$	0	$i = 45$
ϖ_i	$i-31$	$i-34$	$i-42$	$i-41$	$54-i$	0	$i = 46, 47$
ϖ_i	$i-28$	$i-31$	$i-39$	$i-38$	$i-47$	0	$i = 48$
ϖ_i	21	18	10	11	$50-i$	z_6	$i = 49, 50$

where $z_6 = \begin{cases} 1, & \text{if } i = 22, 33, 50; \\ 0, & \text{otherwise.} \end{cases}$

Given locations $l(\varpi|ls)$ of each node of graph of Ritonavir COVID antiviral drug structure is distinct and fulfill the definitions of partition locating set. This proved that the partition locating number $pln(G_{\text{Ritonavir}}) \leq 6$ of graph of Ritonavir COVID antiviral drug structure.

Hence, proved that $pln(G_{\text{Ritonavir}}) \leq 6$. □

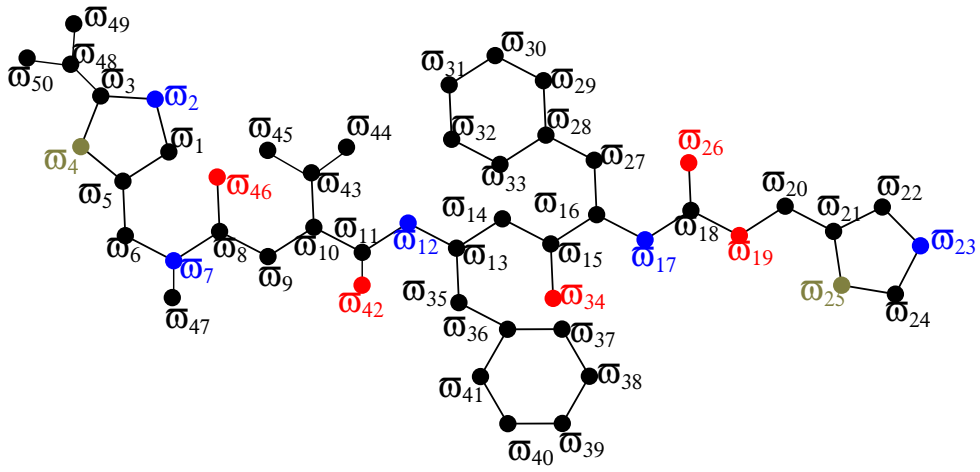

Figure 7. Ritonavir COVID antiviral drug structure.

3. Conclusions

As we can see from our main results section, the partition dimension of arbidol, remdesivir is either four or less, while chloroquine, hydroxy-chloroquine, thalidomide, and theaflavin can be three subsets of their partition resolving sets. The vertex set of ritonavir can be partitioned into either six or less than six subsets. In short, this article detailed a few COVID-19 antiviral structures in the form of molecular graph theory with the metric of vertices. Moreover, the summary of the main results is given in Table 9.

Table 9. Summary of the results.

G	pln
G_{Arbidol}	≤ 4
$G_{\text{Chloroquine}}$	3
G_{Hydroxy}	3
$G_{\text{Thalidomide}}$	3
$G_{\text{Theaflavin}}$	3
$G_{\text{Remdesivir}}$	≤ 4
$G_{\text{Ritonavir}}$	≤ 6

References

1. C. Huang, Y. Wang, X. Li, L. Ren, J. Zhao, Y. Hu, et al., Clinical features of patients infected with 2019 novel coronavirus in wuhan, china, *Lancet*, **395** (2020), 497–506. https://doi.org/10.1016/S0140-6736(20)30183-5

2. M. Wang, R. Cao, L. Zhang, X. Yang, J. Liu, M. Xu, et al., Remdesivir and chloroquine effectively inhibit the recently emerged novel coronavirus (2019-nCoV) in vitro, *Cell Res.*, **30** (2020), 269–271. https://doi.org/10.1038/s41422-020-0282-0
3. D. Zhou, S. Dai, Q. Tong, COVID-19: a recommendation to examine the effect of hydroxychloroquine in preventing infection and progression, *J. Antimicrob. Chemother.*, **75** (2020), 1667–1670. https://doi.org/10.1093/jac/dkaa114
4. J. Lung, Y. Lin, Y. Yang, Y. Chou, L. Shu, Y. Cheng, et al., The potential chemical structure of anti-SARS-CoV-2 RNA-dependent RNA polymerase, *J. Med. Virol.*, **92** (2020), 693–697. https://doi.org/10.1002/jmv.25761
5. J. S. Morse, T. Lalonde, S. Xu, W. R. Liu, Learning from the past: Possible urgent prevention and treatment options for severe acute respiratory infections caused by 2019-nCoV, *ChemBioChem*, **21** (2020), 730–738. https://doi.org/10.1002/cbic.202000047
6. X. Xu, P. Chen, J. Wang, J. Feng, H. Zhou, X. Li, et al., Evolution of the novel coronavirus from the ongoing wuhan outbreak and modeling of its spike protein for risk of human transmission, *Sci. China Life Sci.*, **63** (2020), 457–460. https://doi.org/10.1007/s11427-020-1637-5
7. T. K. Warren, R. Jordan, M. K. Lo, A. S. Ray, R. L. Mackman, V. Soloveva, et al., Therapeutic efficacy of the small molecule GS-5734 against ebola virus in rhesus monkeys, *Nature*, **531** (2016), 381–385. https://doi.org/10.1038/nature17180
8. A. Savarino, L. D. Trani, I. Donatelli, R. Cauda, A. Cassone, New insights into the antiviral effects of chloroquine, *Lancet Infect. Dis.*, **6** (2006), 67–69. https://doi.org/10.1016/S1473-3099(06)70361-9
9. Y. Yan, Z. Zou, Y. Sun, X. Li, K. F. Xu, Y. Wei, et al., Anti-malaria drug chloroquine is highly effective in treating avian influenza a h5n1 virus infection in an animal model, *Cell Res.*, **23** (2013), 300–302. https://doi.org/10.1038/cr.2012.165
10. Johnson & Johnson is already ramping up production on its $1 billion coronavirus vaccine. Available from: https://www.forbes.com/sites/thomasbrewster/2020/03/30/johnson–johnson-is-already-ramping-up-production-on-its-1-billion-coronavirus-vaccine/?sh=2a66d09aaa66.
11. Z. F. Yang, L. P. Bai, W. Huang, X. Li, S. Zhao, N. Zhong, et al., Comparison of in vitro antiviral activity of tea polyphenols against influenza a and b viruses and structure–activity relationship analysis, *Fitoterapia*, **93** (2014), 47–53. https://doi.org/10.1016/j.fitote.2013.12.011
12. P. Chowdhury, M. Sahuc, Y. Rouillé, C. Rivière, N. Bonneau, A. Vandeputte, et al., Theaflavins, polyphenols of black tea, inhibit entry of hepatitis c virus in cell culture, *PLOS One*, **13** (2018), e0198226. https://doi.org/10.1371/journal.pone.0198226
13. A. Ali, W. Nazeer, M. Munir, S. M. Kang, M-polynomials and topological indices of zigzagand rhombic benzenoid systems, *Open Chem.*, **16** (2018), 122–135. https://doi.org/10.1515/chem-2018-0010
14. M. K. Jamil, M. Imran, K. A. Sattar, Novel face index for benzenoid hydrocarbons, *Mathematics*, **8** (2020), 312. https://doi.org/10.3390/math8030312
15. M. K. Siddiqui, M. Naeem, N. A. Rahman, M. Imran, Computing topological indices of certain networks, *J. Optoelectron. Adv. Mater.*, **18** (2016), 9–10.

16. M. Nadeem, M. Azeem, H. A. Siddiqui, Comparative study of zagreb indices for capped, semi-capped, and uncapped carbon nanotubes, *Polycyclic Aromat. Compd.*, **2021** (2020), 1–18. https://doi.org/10.1080/10406638.2021.1890625

17. M. F. Nadeem, M. Imran, H. M. A. Siddiqui, M. Azeem, A. Khalil, Y. Ali, Topological aspects of metal-organic structure with the help of underlying networks, *Arabian J. Chem.*, **14** (2021), 103157. https://doi.org/10.1016/j.arabjc.2021.103157

18. A. N. A. Koam, A. Ahmad, M. E. Abdelhag, M. Azeem, Metric and fault-tolerant metric dimension of hollow coronoid, *IEEE Access*, **9** (2021), 81527–81534. https://doi.org/10.1109/ACCESS.2021.3085584

19. A. Ahmad, A. N. A. Koam, M. H. F. Siddiqui, M. Azeem, Resolvability of the starphene structure and applications in electronics, *Ain Shams Eng. J.*, **13** (2022), 101587. https://doi.org/10.1016/j.asej.2021.09.014

20. M. Azeem, M. F. Nadeem, Metric-based resolvability of polycyclic aromatic hydrocarbons, *Eur. Phys. J. Plus*, **136** (2021), 395. https://doi.org/10.1140/epjp/s13360-021-01399-8

21. Z. Hussain, M. Munir, M. Choudhary, S. M. Kang, Computing metric dimension and metric basis of 2*d* lattice of alpha-boron nanotubes, *Symmetry*, **10** (2018), 300. https://doi.org/10.3390/sym10080300

22. S. Imran, M. K. Siddiqui, M. Hussain, Computing the upper bounds for the metric dimension of cellulose network, *Appl. Math. E-notes*, **19** (2019), 585–605.

23. A. N. A. Koam, A. Ahmad, Barycentric subdivision of cayley graphs with constant edge metric dimension, *IEEE Access*, **8** (2020), 80624–80628. https://doi.org/10.1109/ACCESS.2020.2990109

24. X. Liu, M. Ahsan, Z. Zahid, S. Ren, Fault-tolerant edge metric dimension of certain families of graphs, *AIMS Math.*, **6** (0202), 1140–1152. http://dx.doi.org/2010.3934/math.2021069

25. J. B. Liu, Z. Zahid, R. Nasir, W. Nazeer, Edge version of metric dimension anddoubly resolving sets of the necklace graph, *Mathematics*, **6** (2018), 243. https://doi.org/10.3390/math6110243

26. H. Raza, Y. Ji, Computing the mixed metric dimension of a generalized petersengraph $p(n, 2)$, *Front. Phys.*, **8** (2020), 211. https://doi.org/10.3389/fphy.2020.00211

27. M. F. Nadeem, M. Azeem, A. Khalil, The locating number of hexagonal möbius ladder network, *J. Appl. Math. Comput.*, **66** (2021), 149–165. https://doi.org/10.1007/s12190-020-01430-8

28. M. Ahsan, Z. Zahid, S. Zafar, A. Rafiq, M. Sarwar Sindhu, M. Umar, Computing the edge metric dimension of convex polytopes related graphs, *J. Math. Comput. Sci.*, **22** (2021), 174–188. http://dx.doi.org/10.22436/jmcs.022.02.08

29. A. Ahmad, M. Baca, S. Sultan, Minimal doubly resolving sets of necklace graph, *Math. Rep.*, **20** (2018), 123–129.

30. T. Vetrik, A. Ahmad, Computing the metric dimension of the categorial product of graphs, *Int. J. Comput. Math.*, **94** (2017), 363–371. https://doi.org/10.1080/00207160.2015.1109081

31. A. Ahmad, S. Sultan, On minimal doubly resolving sets of circulant graphs, *Acta Mech. Slovaca*, **20** (2017), 6–11. https://doi.org/10.21496/ams.2017.002

32. A. Ahmad, M. Imran, O. Al-Mushayt, S. A. H. Bokhary, On the metric dimension of barcycentric subdivision of cayley graphs $cay(z_n \oplus z_m)$, *Miskolc Math. Notes*, **16** (2015), 637–646. https://doi.org/10.18514/MMN.2015.1192
33. J. B. Liu, M. F. Nadeem, M. Azeem, Bounds on the partition dimension of convex polytopes, *Comb. Chem. Throughput Screening*, **25** (2020), 547–553. https://doi.org/10.2174/1386207323666201204144422
34. M. Azeem, M. Imran, M. F. Nadeem, Sharp bounds on partition dimension of hexagonal mobius ladder, *J. King Saud Univ. Sci.*, **34** (2022), 101779. https://doi.org/10.1016/j.jksus.2021.101779
35. N. Mehreen, R. Farooq, S. Akhter, On partition dimension of fullerene graphs, *AIMS Math.*, **3** (2018), 343–352. http://dx.doi.org/10.3934/Math.2018.3.343
36. A. Shabbir, M. Azeem. On the partition dimension of tri-hexagonal alpha-boron nanotube, *IEEE Access*, **9** (2021), 55644–55653. https://doi.org/10.1109/ACCESS.2021.3071716
37. M. K. Siddiqui, M. Imran, Computing the metric and partition dimension of h-naphtalenic and vc5c7 nanotubes, *J. Optoelectron. Adv. Mater.*, **17** (2015), 790–794.
38. H. M. A. Siddiqui, M. Imran, Computing metric and partition dimension of 2-dimensional lattices of certain nanotubes, *J. Comput. Theor. Nanosci.*, **11** (2014), 2419–2423. https://doi.org/10.1166/jctn.2014.3656
39. E. C. M. Maritz, T. Vetrík, The partition dimension of circulant graphs, *Quaestiones Math.*, **41** (2018), 49–63. https://doi.org/10.2989/16073606.2017.1370031
40. Z. Hussain, S. Kang, M. Rafique, M. Munir, U. Ali, A. Zahid, et al., Bounds for partition dimension of m-wheels, *Open Phys.*, **17** (2019), 340–344. https://doi.org/10.1515/phys-2019-0037
41. Amrullah, E. Baskoro, R. Simanjuntak, S. Uttunggadewa, The partition dimension of a subdivision of a complete graph, *Procedia Comput. Sci.*, **74** (2015), 53–59. https://doi.org/10.1016/j.procs.2015.12.075
42. C. Wei, M. F. Nadeem, H. M. A. Siddiqui, M. Azeem, J. B. Liu, A. Khalil, On partition dimension of some cycle-related graphs, *Mathematical Problems in Engineering*, **2021** (2021), 4046909. https://doi.org/10.1155/2021/4046909
43. J. Santoso, Darmaji, The partition dimension of cycle books graph, *J. Phys. Conf. Ser.*, **974** (2018), 012070.
44. Darmaji, R. Alfarisi, On the partition dimension of comb product of path and complete graph, in *AIP Conference Proceedings*, (2017), 020038. https://doi.org/10.1063/1.4994441
45. A. Nadeem, A. Kashif, S. Zafar, Z. Zahid, On 2-partition dimension of the circulant graphs, *J. Intell. Fuzzy Syst.*, **40** (2021), 9493–9503. https://doi.org/10.3233/JIFS-201982
46. P.J. Slater, Leaves of trees, Proceeding of the 6th Southeastern Conference on Combinatorics, Graph Theory, and Computing, *Congr. Numerantium*, **14** (1975), 549–559.
47. F. Harary, R. A. Melter, On the metric dimension of a graph, *Ars Comb.*, **2** (1976), 191–195.
48. G. Chartrand, E. Salehi, P. Zhang, The partition dimension of graph, *Aequationes Math.*, **59** (2000), 45–54. https://doi.org/10.1007/PL00000127

49. G. Chartrand, L. Eroh, M. A. O. Johnson, R. Ortrud, Resolvability in graphs and the metric dimension of a graph, *Discrete Appl. Math.*, **105** (2000), 99–113. https://doi.org/10.1016/S0166-218X(00)00198-0
50. S. Khuller, B. Raghavachari, A. Rosenfeld, Landmarks in graphs, *Discrete Appl. Math.*, **70** (1996), 217–229.
51. A. Sebö, E. Tannier, On metric generators of graphs, *Math. Oper. Res.*, **29** (2004), 383–393. https://doi.org/10.1287/moor.1030.0070
52. M. F. Nadeem, M. Hassan, M. Azeem, S. Ud-Din Khan, M. R. Shaik, M. A. F. Sharaf, et al., Application of resolvability technique to investigate the different polyphenyl structures for polymer industry, *J. Chem.*, **2021** (2021), 6633227. https://doi.org/10.1155/2021/6633227
53. J. Caceres, C. Hernando, M. Mora, I. M. Pelayo, M. L. Puertas, C. Seara, et al., On the metric dimension of cartesian product of graphs, *SIAM J. Discrete Math.*, **21** (2007), 423–441. https://doi.org/10.1137/050641867
54. Z. Beerliova, F. Eberhard, T. Erlebach, A. Hall, M. Hoffmann, M. Mihalak, et al., Network discovery and verification, *IEEE J. Selected Areas in Commun.*, **24** (2006), 2168–2181. https://doi.org/10.1109/JSAC.2006.884015
55. V. Chvatal, Mastermind, *Combinatorica*, **3** (1983), 325–329. https://doi.org/10.1007/BF02579188
56. R. A. Melter, I. Tomescu, Metric bases in digital geometry, *Comput. Visual Graphics Image Process.*, **25** (1984), 113–121. https://doi.org/10.1016/0734-189X(84)90051-3
57. C. Hernando, M. Mora, P. J. Slater, D. R. Wood, Fault-tolerant metric dimension of graphs, *Convexity Discrete Struct.*, **5** (2008), 81–85.
58. J. Wei, M. Cancan, A. Rehman, M. Siddiqui, M. Nasir, M. Younas, et al., On topological indices of remdesivir compound used in treatment of corona virus (COVID 19), *Polycyclic Aromat. Compd.*, **2021** (2021), 1–19. https://doi.org/10.1080/10406638.2021.1887299
59. S. Mondal, N. De, A. Pal, Topological indices of some chemical structures applied for the treatment of COVID-19 patients, *Polycyclic Aromat. Compd.*, **42** (2022), 1–15. https://doi.org/10.1080/10406638.2020.1770306

AIMS Press